# Photoredox Oxidation of Alkanes by Monometallic Copper-Oxygen Complexes Using Visible Light Including One Sun Illumination

Daniel L. Nascimento, David Gygi, Matthew C. Drummer, Miguel I. Gonzalez, Shao-Liang Zheng and Daniel G. Nocera*

Department of Chemistry and Chemical Biology, Harvard University, Cambridge, Massachusetts 02138, United States

ABSTRACT: Oxygenation of hydrocarbons offers versatile catalytic routes to more valuable compounds, such as alcohols, aldehydes and ketones. Despite the importance of monometallic copper-oxygen species as hydroxylating agents in biology, few synthetic model compounds are known to react with unactivated hydrocarbons owing to high C–H bond dissociation energies. To overcome this challenge, the photoredox chemistry of monometallic copper (pyrazolyl)borate complexes coordinated by chlorate has been explored in the presence of $C_1$–$C_6$ alkanes with BDEs ≥ 93 kcal/mol. Ethane is photooxidized at room temperature under $N_2$ with yields of 15–30%, which increases to 77% for the most oxidizing tris(3,5-trifluoromethyl-pyrazolyl)borate complex (**Cu-3**). This complex also promotes the photooxidation of methane to methanol at significant yield (38%) when the photoredox reaction is run under aerobic conditions. Ligand modification alters reaction selectivity by tuning the redox potential. The ability to activate 1° C–H bonds of $C_1$–$C_6$ light alkanes using visible light is consistent with the photogeneration of a powerfully oxidizing copper-oxyl, which is supported by photocrystallographic studies of the (pyrazolyl)borate chlorate complex. Mechanistic studies are consistent with hydrogen atom abstraction of the C–H bond by the copper-oxyl intermediate. We demonstrate for **Cu-3** with hexane as an exemplar, that the photoredox chemistry may be achieved under solar conditions of 1-sun illumination.

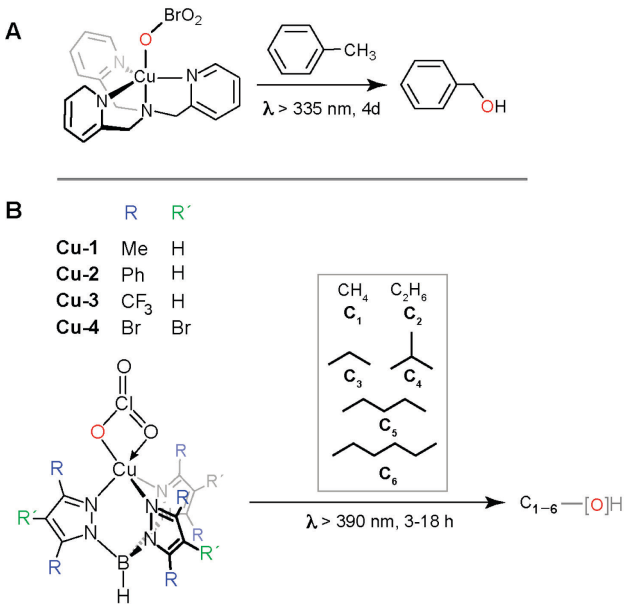


**Figure 1.** Photooxidation chemistry of **(A)** Cu tris(2-pyridylmethyl)-amine (ref 47) and **(B)** Cu (pyrazolyl)borate complexes (this study).

Oxidation of light alkanes into value-added liquid products is an important target for instituting sustainable chemical processes.[1] Current methods for achieving such transformations require harsh energy inputs due to the inertness of the C–H bonds. Conversely, in nature, hydroxylation of alkanes is accomplished under mild conditions at the mono- and multi-metallic copper centers of oxygenases.[2–6] The oxidation chemistry is induced when the Cu(II)-(hydr)oxo formal oxidation state is raised one level to Cu(III)-oxo, which may often be better formulated as a Cu(II)–oxyl radical (i.e., $Cu^{II}$–O•) based on electronic considerations embodied by the "oxo wall".[7] For example, in the most investigated multi-copper site—the particulate methane monooxygenase (pMMO)[8,9]—a putative $Cu^{II}$–O• in terminal or bridging coordination geometry is thought to be the oxidizing agent of methane.[10,11]

The prevalence of $Cu^{II}$–O• as a hydroxylating agent of C–H bonds in biology has prompted efforts devoted to reproducing this intermediate in homogeneous complexes[12–16] and heterogeneous[17–23] materials. In contrast to the limited activity of mononuclear $Cu^{II}O$–O• and $Cu^{II}O$–OH adducts towards substrates,[24–31] $Cu^{II}$–O• intermediates have been proposed to activate strong C–H bonds.[32–34] Traditional approaches to generating mononuclear reactive copper species generally involve the reaction of Cu with reactive oxidants such as $H_2O_2$ and PhIO.[34–36] The resulting copper intermediates of these oxidations are extremely reactive, thus requiring low temperatures for their observation.[37–45]

As an alternative strategy to thermal generation, reactive copper-based oxo intermediates may be accessed by photochemical and electrochemical methods.[46] Irradiation of a tetradentate Cu complex bound by bromate with >335 nm light over the course of 4 days leads to the

generation of a Cu intermediate that is competent towards C–H oxidation (Figure 1A).[47] Kinetic isotope measurements revealed that C–H cleavage is the rate determining step of the reaction, likely a result of the relative stability of the Cu-oxo moiety as evidenced by the inability to oxidize light alkanes such as pentane (BDE = 98 kcal/mol). For the case of the late transition metals, more reactive metal-oxos may be manifest in a pseudo-tetrahedral ligand field.[48,49] Accordingly, we were intrigued with the ligand field offered by tris-pyrazolylborate (**Tp$^{R}$**),[50] which has been employed to mimic the coordination environment of blue[51] and green[52] copper proteins. We now report that the **Tp$^{R}$** complexes bearing a chlorate ligand, **Cu-1** to **Cu-4** (Figure 1B), are active C–H photooxidation catalysts. All complexes are capable of photooxidizing light alkanes at room temperature with yields varying between 16–77%, including the photooxidization of methane to methanol by the best-performing **Cu-3** complex, (6% anaerobic, 38% aerobic). The **Tp$^{R}$** ligand field can be modified to tune the redox potential of Cu to be varied by >400 mV. The higher yields and greater oxidation of 1° C–H bonds are result of the increased oxidizing power of the copper center, consistent with the photogeneration of a powerfully oxidizing copper-oxyl. We demonstrate for **Cu-3** with hexane as an exemplar, that the photoredox chemistry may be achieved under solar conditions of 1-sun illumination.

In the absence of a stable $Cu(ClO_3)_2 \bullet xH_2O$ salt,[53] **Cu-1** to **Cu-4** were obtained from a metathesis reaction between $CuBr_2$ and $AgClO_3$. Single crystals of complexes suitable for X-ray diffraction analysis afforded the structures shown in Figure S1 (and Table S1). The Cu$^{II}$ site adopts a pseudo-square pyramidal geometry with chlorate adopting an $\kappa^2$ ligation. NMR spectra (Figure S2) are consistent with a paramagnetic ground state, as confirmed by EPR spectra, which display an axially symmetric Cu$^{II}$ with $g_\perp$ ranging between 2.06–2.07 and $g_{||}$ between 2.29–2.34 (Figure S3). An ill-resolved 4-line signal arising from coupling to $^{63,65}$Cu ($I$ = 3/2) is observed with no distinguishable hyperfine coupling to the N atoms of the **Tp$^{R}$** ligands. A $g_\perp < g_{||}$ is suggestive of an unpaired electron in the $d_{x^2-y^2}$ orbital of the ground state.[54] The Cu$^{II}$/Cu$^{I}$ oxidation-reduction potential is significantly modified by the **Tp$^{R}$** ligand, which was assessed using the Cu$^{I}$-$CH_3CN$ adducts (**Cu-5** to **Cu-8**, Chart S1) so as to avoid the electrochemical irreversibility of the chlorate ligand (Figure S4). A potential ranging from –0.05 vs $Fc^+/Fc$ for the most reducing ligand (**Tp$^{Me}$**) to 0.5 V for the most oxidizing ligand **(Tp$^{CF_3}$**).

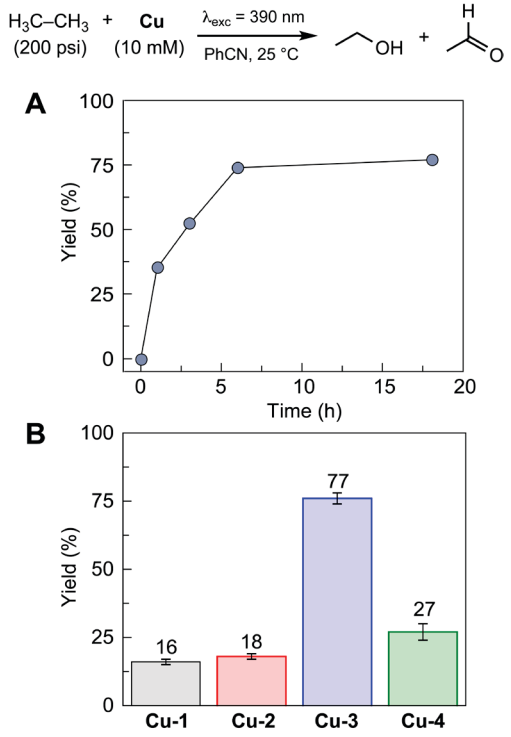


**Figure 2.** (**A**) Rate of ethane photooxidation by **Cu-3** over time. (**B**) Yield of oxidized products (Table S3) at 18 h for **Cu-1** to **Cu-4**.

Complexes **Cu-1** to **Cu-4** exhibit a weak absorption in the red spectral region (Figure S5), consistent with d–d transitions, and a rising absorption in the UV spectral region. Irradiation into the UV absorption band of solutions of the complexes (10 mM Cu) and alkane substrates under $N_2$ with a 390 nm Kessil LED lamp leads to a prompt and facile photoreactivity. Complex **Cu-3** was used to investigate the reaction profile for the oxidation of ethane (Figure 2A), which contains strong primary C–H bonds (BDE = 101 kcal/mol). Owing to the low solubility of ethane in organic solvents,[55] the photoredox reaction was

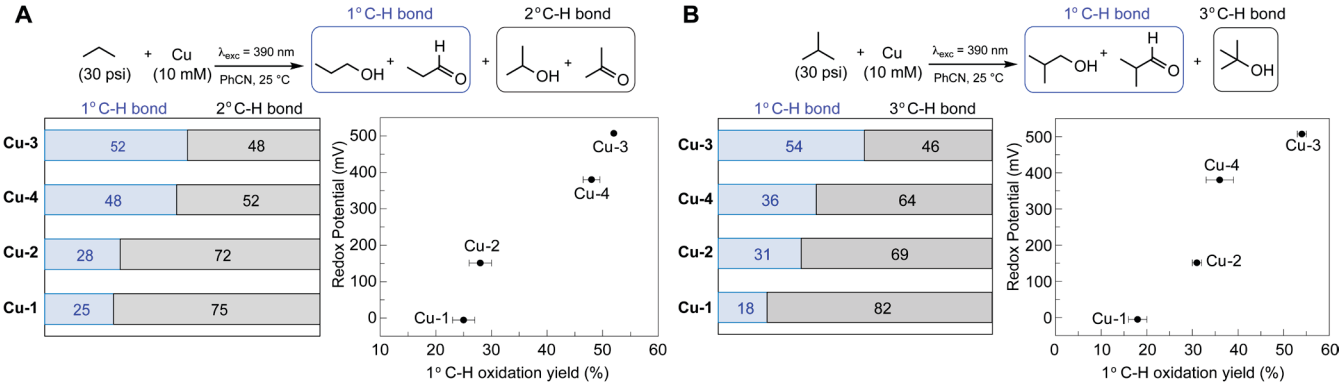


**Figure 3**. Photooxidation products of (**A**) propane (Table S4) and (**B**) isobutane (Table S5) by **Cu-1** to **Cu-4**. Horizontal bar graphs show the selectivity for oxidized products generated from 1° vs 2° or 3° C–H bond sites. Scatter plots show the relationship between redox potential vs product yield generated from oxidation of 1° C–H sites.

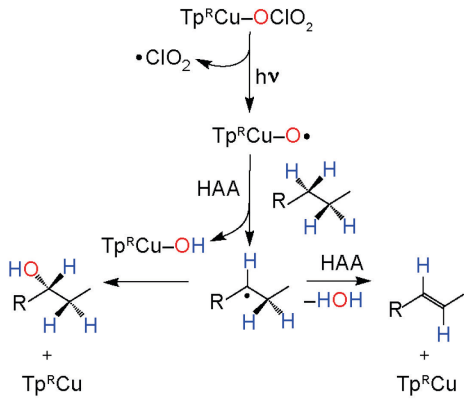


**Figure 4**. Proposed photoredox mechanism of alkane oxidation by copper complexes, **Cu-1** to **Cu-4**. The mechanism is consistent with the chemical generation of the oxyl intermediate and is supported by DFT calculations from ref 32.

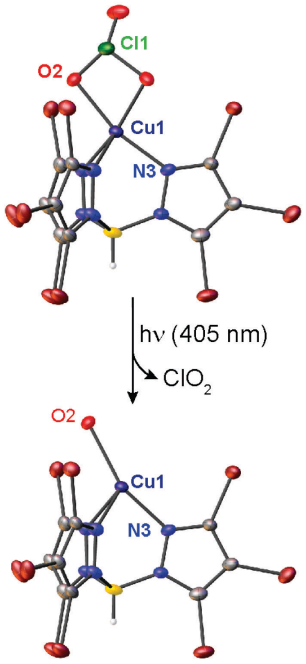


**Figure 5**. Photocrystallographic characterization of a single crystal of **Cu-4** upon $ClO_2$ photoelimination, as determined from X-ray diffraction data collected at 100 K. The H atom was not located in the electron density difference map. In addition to the Cu and O atom labels, burnt orange, yellow, blue, gray, and white spheres represent Br, B, N, C and H atoms, respectively. Photoeliminated $ClO_2$ was not located in the Fourier photodifference map, indicating its diffusion from the crystal during irradiation.

conducted in a high-pressure reactor. The rate of product formation increases over 5 h to a yield of 75%, after which the yield increases incrementally to 77% (Figure 2A). All complexes show conversion of ethane to ethanol and acetaldehyde, as determined by a GC-FID assay; no acetic acid was detected. Control experiments with solutions of the $\mathbf{Tp^{Ph}}$ ligand, $Cu(ClO_3)_2$ or solutions of $\mathbf{Tp^RCuClO_3}$ in the absence of light or ethane show no reaction. Complex **Cu-1**, which has a similar steric environment compared to **Cu-3**, showed reduced ethane oxidation (16%, Figure 2B), indicating that differences in the electronic properties of $CH_3$ vs $CF_3$ substituents lead to differences in reactivity. We postulate that a complex bearing electron withdrawing groups on the $\mathbf{Tp^R}$ backbone (R = $CF_3$ and Br, **Cu-3** and **Cu-4**, respectively) engenders a weaker Cu–O bond and higher oxidizing power at the Cu center, thus increasing overall conversion yields. Complex **Cu-2** exhibited similar photoredox activity (18%) as **Cu-1**, indicating that the steric bulk of ancillary phenyl rings on the ligand does not shield the copper center from ethane. **Cu-4** furnished intermediate yields.

The ability to activate the strong C–H bond of ethane prompted us to examine other light alkanes with the 2° and 3° C–H bonds of propane and isobutane as targets. Because of the greater solubility of these gases in organic solvents, a pressure of 30 psi was used for these substrates and reaction times were decreased to 3 h. Figure 3A shows the selectivity for oxidation of 1° vs 2° sites of propane for each complex. The more strongly oxidizing **Cu-3** complex results in greater oxidation of 1° C–H sites relative to 2° C–H sites. The yield of oxidation at the 1° site of substrate increases monotonically with an increase in the Cu(II) redox potential. A similar trend is observed for the oxidation of the 1° vs 3° C–H bonds of isobutane (Figure 3B). The regioselectivity for activation of the 1° C–H bond exhibits a marginal preference enhanced normalized for the number of C–H bonds, establishing that C–H activation is under thermodynamic vs kinetic control.

We performed further experiments using liquid alkanes (i) for comparison to results when the $Cu^{II}$–O• intermediate is generated chemically, and (ii) to facilitate the accurate measurement of quantum yields and kinetic isotope effects. The photooxidation of hexane with 390-nm excitation results in the primary production of alkene and ketone, which results from the over-oxidation of the alcohol (Table S6). A similar result is obtained for pentane (Table S7). Optimized conditions are obtained when the alkane is in excess; a considerable decrease in yield is observed for stoichiometric amounts of substrate owing to photodegradation of the Cu complexes by reaction with solvent. We note that the product distributions for alkene and ketone are similar to that when the $Cu^{II}$–O• intermediate is generated from the $Tp Cu^{I}$ acetonitrile adduct (**Cu-8**) using $H_2O_2$ as an oxidant.[32] The similar product distributions between the photoredox and chemical systems are noteworthy, as the latter cannot derive reactivity from chlorine-based radicals, suggesting that the chemistry is not driven by •$ClO_2$. Consistent with this contention, the disparate photoactivity amongst the Cu complexes alludes to $Cu^{II}$–O• as the reactive intermediate as opposed to •$ClO_2$, which would have no redox dependence on C–H activation.[56] To further probe this issue, •Cl,[56] •$ClO_2$[57] and •$ClO_3$[58] were photogenerated by established methods in the presence of hexane. The reaction yields and product distributions did not coincide with those of **Cu-1** to **Cu-4** (Table S6). When the photoredox reaction was performed for **Cu-3** in the presence of 1,4-cyclohexadiene and styrene, benzene was observed for the former substrate (Figure S12A) and no styrene oxide was detected for the latter substrate (Figure S12B). These results are consistent

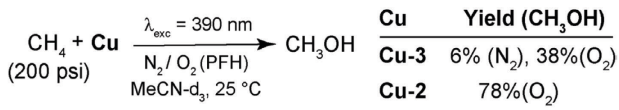


**Scheme 1.** Catalytic methane oxidation by **Cu-2** and **Cu-3**.

with a mechanism that is radical-based as opposed to O-atom transfer. To rule out the involvement of a bimetallic intermediate as the active species, photochemical experiments of several $\mathbf{Tp^{Me}_2Cu_2O_{1\text{-}2}}$ complexes (Chart S1) in the presence of hexane were performed. No hexane oxidation products were detected, consistent with a monometallic $Cu^{II}$–$O^{\bullet}$ as the reactive intermediate.

The photooxidation quantum yields for the four Cu complexes range from 0.6–2.5% (Table S8), with the most oxidizing **Cu-3** complex exhibiting the highest quantum yield. The appreciable quantum yield prompted us to investigate whether the photoredox chemistry could be driven with solar light. Indeed, **Cu-3** exhibited photooxidation yields of 34% for hexane oxidation when irradiated under 1-sun illumination vs 42% for irradiation with a 390 nm Kessil lamp (Table S6).

A mechanism consistent with photooxidation of alkane is shown in Figure 4. This mechanism is coincident with that proposed for the generation of the $Cu^{II}$–$O^{\bullet}$ by $H_2O_2$ oxidation of the $TpCu^{I}$ center.[32,59] The photogenerated $Cu^{II}$–$O^{\bullet}$ undergoes hydrogen atom abstraction (HAA) from alkane (RH) to form $Cu^{II}$–OH and $R^{\bullet}$. A kinetic isotope effect of 3.6 to 4.3, when the Cu complexes were irradiated in the presence of toluene and toluene-$d_8$, establishes significant C–H cleavage in the transition state (Table S8). A rebound mechanism transfers the OH group back to the alkyl radical to yield ROH and $Tp^{R}Cu$. Alternatively, as has been proposed based on DFT calculations,[32] the $TpCu^{II}(OH)$ center has sufficient radical character on oxygen to promote an ensuing HAA to furnish alkene.

The generation of $Cu^{II}$–$O^{\bullet}$ upon $ClO_2$ photoelimination is supported by photocrystallography measurements of single crystals of **Cu-4** irradiated with 405 nm light at 100 K. Comparison of the dark and photoinduced structures reveals that photolysis of the complex leads to elimination of $ClO_2$ and formation of the Cu–O motif (Figure 5). The resulting photolyzed structure (13.7% conversion) shows a terminal oxygen at d(Cu1–O2) = 2.32(6) Å that is bent and elongated, likely a result of crystal packing. Selected photocrystallography bond and angle metrics are listed in Table S2. Production of the mono-oxo Cu photoproduct is also supported by matrix-assisted laser ionization (MALDI) measurements (Figure S6).

Of the light alkanes, methane is an important target substrate owing to a keen interest in its oxidation as well as presenting the most reticent 1° C–H bond to activate (BDE = 105 kcal/mol).[60] Photo-oxidation experiments of methane with the best-performing complex, **Cu-3**, were conducted under similar conditions as those used for the other light alkanes (Scheme 1). Irradiation of 10 mM **Cu-3** under $N_2$ in MeCN-$d_3$ over 18 h in the presence of 200 psi $CH_4$ at 25 °C showed the formation of methanol in 6% yield as confirmed by $^1$H NMR spectroscopy (Figure S7) and GC-MS (Figure S8). To investigate whether the low yield was a result of over-oxidation (Figure S9), **Cu-3** was irradiated with 390 nm light in the presence of methanol. After 18 h, 60% methanol was consumed (Figure S10) with the detection of CO and $CO_2$ by gas chromatographic analysis of the reaction headspace (Figure S11) and no other C1 products (1% formic, 0% formaldehyde). Repeating this experiment with the less oxidizing **Cu-2** complex showed only 1% methanol consumption, indicating less over-oxidation owing to the reduced oxidizing power of **Cu-2** vs **Cu-3**.

The formation of a Cu-oxyl suggests that the methane oxidation yields could be increased by generating the $Cu^{II}$–$O^{\bullet}$ intermediate under aerobic conditions to initiate a radical chain pathway.[2,57] Indeed, the photooxidation conversion yield of methane to methanol increased significantly under aerobic conditions in perfluorohexane (PFH). Irradiation of 2mM **Cu-2** in $O_2$-saturated PFH over 24 h in the presence of 200 psi $CH_4$ showed the formation of 44% methanol. Increasing the photon flux by approximately ×2 resulted in 78% MeOH yield for **Cu-2** vs 38% for **Cu-3**, confirming the increased selectivity of the former arising from reduced over-oxidation of MeOH. A control reaction with **Cu-2** in the absence of $CH_4$ showed no methanol production. The increased yield of MeOH is consistent with a radical chain mechanism initiated by H• abstraction of methane.[57] With excess oxygen present, the Me• can react with $O_2$ to generate MeOO•, which disproportionates to $O_2$ and MeO•, which then reacts with another equivalent of $CH_4$ to yield MeOH and Me•. The ability to generate MeOH from $CH_4$ at room temperature using visible light highlights the benefits of photoredox methods to generate reactive intermediates that can activate recalcitrant C–H substrates.

The results reported herein establish the utility of photochemistry in achieving the oxidation of alkanes under mild conditions. A pseudo-tetrahedral ligand field around Cu allows alkanes to be photooxidized at room temperature using chlorate as the primary oxidant. A powerfully oxidizing Cu-oxyl intermediate may be generated upon ligand-to-metal charge transfer excitation with visible light, including 1-sun illumination. For the case of liquid alkanes, the results obtained by photoredox parallel those when the Cu-oxyl intermediate is generated chemically from $H_2O_2$. By tuning the oxidizing power of the copper-oxyl with the ancillary ligand field, the level of substrate oxidation may be controlled.

## ASSOCIATED CONTENT

### Supporting Information

Experimental data, crystallographic data, UV-vis, EPR and NMR spectra. This material is available free of charge via the Internet at http://pubs.acs.org. Metrical data and supplementary crystallographic data for the solid-state structures are available from the Cambridge Crystallographic Data Centre under reference numbers CCDC 2364102, 2364103, 2364104, 2354611, 2354612, 2354613, 2354614. These data can be obtained free of charge via www.ccdc.cam.ac.uk/data_request/cif, or by emailing data_request@ccdc.cam.ac.uk, or by contacting The Cambridge Crystallographic Data Centre, 12 Union Road, Cambridge CB2 1EZ, UK; fax: +44 1223 336033.

## AUTHOR INFORMATION


### Corresponding Author

**Daniel G. Nocera** – Department of Chemistry and Chemical Biology, Harvard University, Cambridge, Massachusetts 02138, United States; orcid.org/0000-0001-5055-320X; Email: dnocera@fas.harvard.edu.

### Authors

**Daniel L. Nascimento** – Department of Chemistry and Chemical Biology, Harvard University, Cambridge, Massachusetts 02138, United States; orcid.org/0000-0002-9363-2175.

**David Gygi** – Department of Chemistry and Chemical Biology, Harvard University, Cambridge, Massachusetts 02138, United States; orcid.org/0000-001-9070-4973.

**Matthew C. Drummer**– Department of Chemistry and Chemical Biology, Harvard University, Cambridge, Massachusetts 02138, United States.

**Miguel I. Gonzalez** – Department of Chemistry and Chemical Biology, Harvard University, Cambridge, Massachusetts 02138, United States; orcid.org/0000-0003-4250-9035.

Present Addresses – Department of Chemistry, Dartmouth College, Burke Laboratory, Hanover, NH 03755.

**Shao-Liang Zheng** – Department of Chemistry and Chemical Biology, Harvard University, Cambridge, Massachusetts 02138, United States; orcid.org/0000-0002-6432-9943.


### Notes

The authors declare no competing financial interest.

## ACKNOWLEDGMENT


This research was supported by the National Science Foundation (NSF) Division of Chemistry under the grant number CHE-2243724. NSF's ChemMatCARS Sector 15 at the Advanced Photon Source, Argonne National Laboratory, is supported by the Divisions of Chemistry (CHE) and Materials Research (DMR), NSF, under grant number NSF/CHE-1834750. Use of the Advanced Photon Source, an Office of Science User Facility operated for the U.S. Department of Energy (DOE) Office of Science by Argonne National Laboratory, was supported by the DOE under Contract No. DE-AC02-06CH11357. We thank Dr. Jesse Gordon for the help with collecting the XRD data.


## REFERENCES


(1) Tang, X.; Jia, X.; Huang, Z. Challenges and Opportunities for Alkane Functionalization Using Molecular Catalysts. *Chem. Sci.* **2018**, *9*, 288–299.

(2) Kitajima, N.; Moro-oka, Y. Copper-Dioxygen Complexes. Inorganic and Bioinorganic Perspectives. *Chem. Rev.* **1994**, *94*, 737–757.

(3) Solomon, E. I.; Sundaram, U. M.; Machonkin, T. E. Multicopper Oxidases and Oxygenases. *Chem. Rev.* **1996**, *96*, 2563–2606.

(4) Tinberg, C. E.; Lippard, S. J. Dioxygen Activation in Soluble Methane Monooxygenase. *Acc. Chem. Res.* **2011**, *44*, 280–288.

(5) Tolman, W. B. Making and Breaking the Dioxygen O–O Bond: New Insights from Studies of Synthetic Copper Complexes. *Acc. Chem. Res.* **1997,** *30*, 227–237.

(6) Woodland, M. P.; Dalton, H. Purification and Characterization of Component A of the Methane Monooxygenase from Methylococcus Capsulatus (Bath). *J. Biol. Chem.* **1984**, *259*, 53–59.

(7) Winkler, J. R.; Gray, H. B. Electronic Structures of Oxo-Metal Ions. In *Molecular Electronic Structures of Transition Metal Complexes I. Structure and Bonding;* Mingos, D. M. P.; Day, P.; Dahl, J. P., Eds.; Springer: New York NY; vol. 142, pp 17–28 (2012).

(8) Jodts, R. J.; Ross, M. O.; Koo, C. W.; Doan, P. E.; Rosenzweig, A. C.; Hoffman, B. M. Coordination of the Copper Centers in Particulate Methane Monooxygenase: Comparison between Methanotrophs and Characterization of the CuC Site by EPR and ENDOR Spectroscopies. *J. Am. Chem. Soc.* **2021**, *143*, 15358–15368.

(9) Chang**,** W. H.; Lin, H. H.; Tsai, I. K.; Huang, S. H.; Chung, S. C.; Tu, I. P.; Yu**,** S. S. F.; Chan, S. I. Copper Centers in the Cryo-EM Structure of Particulate Methane Monooxygenase Reveal the Catalytic Machinery of Methane Oxidation. *J. Am. Chem. Soc.* **2021**, *143*, 9922–9932.

(10) Ross M. O.; MacMillan, F.; Wang, J.; Nisthal, A.; Lawton, T. J.; Olafson, B. D.; Mayo, S. L.; Rosenzweig, A. C.; Hoffman, B. M. Particulate Methane Monooxygenase Contains Only Mononuclear Copper Centers. *Science* **2019**, *364*, 566–570.

(11) Chen, P. P. Y.; Chan, S. I. Theoretical Modeling of the Hydroxylation of Methane as Mediated by the Particulate Methane Monooxygenase. *J. Inorg. Biochem.* **2006**, *100*, 801–809.

(12) Weaver, J. F.; Hakanoglu, C.; Antony, A.; Asthagiri, A. Alkane Activation on Crystalline Metal Oxide Surfaces. *Chem. Soc. Rev.* **2014**, *43*, 7536–7547.

(13) Citek, C.; Gary, J. B.; Wasinger, E. C.; Stack, T. D. P. Chemical Plausibility of Cu(III) with Biological Ligation in pMMO. *J. Am. Chem. Soc.* **2015**, *137*, 6991–6994.

(14) Gary, J. B.; Citek, C.; Brown, T. A.; Zare, R. N.; Wasinger, E. C.; Stack, T. D. P. Direct Copper(III) Formation from $O_2$ and Copper(I) with Histamine Ligation. *J. Am. Chem. Soc.* **2016**, *138*, 9986–9995.

(15) Cavaliere, V. N.; Mindiola, D. J. Methane: A New Frontier in Organometallic Chemistry. *Chem. Sci.* **2012**, *3*, 3356–3365.

(16) Wang, V. C. C.; Maji, S.; Chen, P. P. Y.; Lee, H. K.; Yu, S. S. F.; Chan, S. I. Alkane Oxidation: Methane Monooxygenases, Related Enzymes, and Their Biomimetics. *Chem. Rev.* **2017**, *117*, 8574–8621.

(17) Qi, Q.; Wang, X.; Chen, L.; Li, B. Methane Dissociation on Pt(111), Ir(111) and PtIr(111) Surface: A Density Functional Theory Study. *Appl. Surf. Sci.* **2013**, *284*, 784–791.

(18) Wang, C. C.; Siao, S. S.; Jiang, J. C. C-H Bond Activation of Methane via s-d Interaction of the $IrO_2$(110) Surface: Density Functional Theory Study. *J. Phys. Chem. C.* **2012**, *116*, 6367–6370.

(19) Pham, T. L. M.; Leggesse, E. G.; Jiang, J. C. Ethylene Formation by Methane Dehydrogenation and C-C Coupling Reaction on a Stoichiometric $IrO_2$(110) Surface – A Density Functional Theory Investigation. *Catal. Sci. Technol.* **2015**, *5*, 4064–4071.

(20) Woertink, J. S.; Smeets, P. J.; Groothaert, M. H.; Vance, M. A.; Sels, B. F.; Schoonheydt, R. A.; Solomon, E. I. A $[Cu_2O]^{2+}$ Core in Cu-ZSM-5, the Active Site in the Oxidation of Methane to Methanol. *Proc. Natl. Acad. Sci. U.S.A.* **2009**, *106*, 18908–18913.

(21) Grundner, S.; Markovits, M. A. C.; Li, G.; Tromp, M.; Pidko, E. A.; Hensen, E. J. M.; Jentys, A.; Sanchez-Sanchez, M.; Lercher, J. A. Single-Site Trinuclear Copper Oxygen Clusters in Mordenite for Selective Conversion of Methane to Methanol. *Nat. Commun.* **2015**, *6*, 7546.

(22) Narsimhan, K.; Iyoki, K.; Dinh, K. Roman-Leshkov, Y. Catalytic Oxidation of Methane into Methanol over Copper-Exchanged Zeolites with Oxygen at Low Temperature. *ACS Cent. Sci.* **2016**, *2*, 424–429.

(23) Mahyuddin, M. H.; Staykov, A.; Shiota, Y.; Yoshizawa, K. Direct Conversion of Methane to Methanol by Metal-Exchanged ZSM-5 Zeolite (Metal = Fe, Co, Ni, Cu). *ACS Catal.* **2016**, *6*, 8321–8331.

(24) Itoh, S. Mononuclear Copper Active-Oxygen Complexes. *Curr. Opin. Chem. Biol.* **2006**, *10*, 115–122.

(25) Diaz, D. E.; Bhadra, M.; Karlin, K. D. Dimethylanilinic N-Oxides and Their Oxygen Surrogacy Role in the Formation of a

Putative High-Valent Copper–Oxygen Species. *Inorg. Chem.* **2019**, *58*, 13746–13750.

(26) Himes, R. A.; Karlin, K. D. Copper–Dioxygen Complex Mediated C–H Bond Oxygenation: Relevance for Particulate Methane Monooxygenase (pMMO). *Curr. Opin. Chem. Biol.* **2009**, *13*, 119–131.

(27) Álvarez, M.; Molina, F.; Fructos, M. R.; Urbano, J.; Álvarez, E.; Sodupe, M.; Lledós, A.; Pérez, P. J. Aerobic Intramolecular Carbon–Hydrogen Bond Oxidation Promoted by Cu(I) Complexes. *Dalton Trans.* **2020**, *49*, 14647–14655.

(28) Conde, A.; Mar Díaz-Requejo, M.; Pérez, P. J. Direct, Copper-Catalyzed Oxidation of Aromatic C–H Bonds with Hydrogen Peroxide Under Acid-Free Conditions. *Chem. Commun.* **2011**, *47*, 8154–8156.

(29) Liu, J. J.; Diaz, D. E.; Quist, D. A.; Karlin, K. D. Copper(I)-Dioxygen Adducts and Copper Enzyme Mechanisms. *Isr. J. Chem.* **2016**, *56*, 9–10.

(30) Elwell, C. E.; Gagnon, N. L.; Neisen, B. D.; Dhar, D.; Spaeth, A. D.; Yee, G. M.; Tolman, W. B. Copper–Oxygen Complexes Revisited: Structures, Spectroscopy, and Reactivity. *Chem. Rev.* **2017,** *117*, 2059–2107.

(31) Donoghue, P. J.; Tehranchi, J.; Cramer, C. J.; Sarangi, R.; Solomon, E. I.; Tolman, W. B. Rapid C–H Bond Activation by a Monocopper(III)–Hydroxide Complex. *J. Am. Chem. Soc.* **2011**, *133*, 17602–17605.

(32) Conde, A.; Vilella, L.; Balcells, D.; Díaz-Requejo, M. M.; Lledós, A.; Pérez, P. J. Introducing Copper as Catalyst for Oxidative Alkane Dehydrogenation. *J. Am. Chem. Soc.* **2013**, *135*, 3887–3896.

(33) Dietl, N.; van der Linde, C.; Schlangen, M.; Beyer, M. K.; Schwarz, H. Diatomic $[CuO]^+$ and Its Role in the Spin-Selective Hydrogen- and Oxygen-Atom Transfers in the Thermal Activation of Methane. *Angew. Chem. Int. Ed.* **2011**, *50*, 4966–4969.

(34) Wu, P.; Zhang, J.; Chen, Q.; Peng, W.; Wang, B. Theoretical Perspective on Mononuclear Copper-Oxygen Mediated C–H and O–H Activations: A Comparison Between Biological and Synthetic Systems. *Chin. J. Catal.* **2022**, *43*, 913–927.

(35) Maiti, D.; Narducci Sarjeant, A. A.; Karlin, K. D. Copper–Hydroperoxo-Mediated N-Debenzylation Chemistry Mimicking Aspects of Copper Monooxygenases. *Inorg. Chem.* **2008**, *47*, 8736–8747.

(36) Jeon, H.; Oh, H.; Hong, S. Synthesis, Characterization and Catalytic Activity of a Mononuclear Nonheme Copper(II)-iodosylbenzene Adduct. *J. Inorg. Biochem.* **2021**, *223*, 111524.

(37) Maiti, D.; Lee, D. H.; Gaoutchenova, K.; Würtele, C.; Holthausen, M. C.; Narducci Sarjeant, A. A.; Sundermeyer, J.; Schindler, S.; Karlin, K. D. Reactions of a Copper(II) Superoxo Complex Lead to C–H and O–H Substrate Oxygenation: Modeling Copper-Monooxygenase C–H Hydroxylation. *Angew. Chem. Int. Ed.* **2007**, *47*, 82–85.

(38) Kim, S.; Ginsbach, J. W.; Lee, J. Y.; Peterson, R. L.; Liu, J. J.; Siegler, M. A.; Sarjeant, A. A.; Solomon, E. I.; Karlin, K. D. Amine Oxidative N-Dealkylation via Cupric Hydroperoxide Cu–OOH Homolytic Cleavage Followed by Site-Specific Fenton Chemistry. *J. Am. Chem. Soc.* **2015**, *137*, 2867–2874.

(39) Choi, Y. J.; Cho, K.-B.; Kubo, M.; Ogura, T.; Karlin, K. D.; Cho, J.; Nam, W. Spectroscopic and Computational Characterization of $Cu^{II}$–OOR (R = H or Cumyl) Complexes Bearing a $Me_6$-tren Ligand. *Dalton Trans.* **2011**, *40*, 2234–2241.

(40) Cramer, C. J.; Tolman, W. B. Mononuclear Cu–$O_2$ Complexes: Geometries, Spectroscopic Properties, Electronic Structures, and Reactivity. *Acc. Chem. Res.* **2007**, *40*, 601–608.

(41) Tano, T.; Ertem, M. Z.; Yamaguchi, S.; Kunishita, A.; Sugimoto, H.; Fujieda, N.; Ogura, T.; Cramer, C. J.; Itoh, S. Reactivity of Copper(II)-Alkylperoxo Complexes. *Dalton Trans.* **2011**, *40*, 10326–10336.

(42) Kitajima, N.; Katayama, T.; Fujisawa, K.; Iwata, Y.; Morooka, Y. Synthesis, Molecular Structure, and Reactivity of (Alkylperoxo)Copper(II) Complex. *J. Am. Chem. Soc.* **1993**, *115*, 7872–7873.

(43) Chen, P.; Fujisawa, K.; Solomon, E. I. Spectroscopic and Theoretical Studies of Mononuclear Copper(II) Alkyl- and Hydroperoxo Complexes: Electronic Structure Contributions to Reactivity. *J. Am. Chem. Soc.* **2000**, *122*, 10177–10193.

(44) Kunishita, A.; Ishimaru, H.; Nakashima, S.; Ogura, T.; Itoh, S. Reactivity of Mononuclear Alkylperoxo Copper(II) Complex. O–O Bond Cleavage and C–H Bond Activation. *J. Am. Chem. Soc.* **2008**, *130*, 4244–4245.

(45) Dhar, D.; Yee, G. M.; Spaeth, A. D.; Boyce, D. W.; Zhang, H.; Dereli, B.; Cramer, C. J.; Tolman, W. B. Perturbing the Copper(III)–Hydroxide Unit through Ligand Structural Variation. *J. Am. Chem. Soc.* **2016**, *138*, 356–368.

(46) Meng, X.; Cui, X.; Rajan, N. P.; Yu, L.; Deng, D.; Bao, X. Direct Methane Conversion under Mild Condition by Thermo-, Electro-, or Photocatalysis. *Chem. Lett.* **2019**, *5*, 2296–2325.

(47) Van Trieste, G. P.; Reibenspies, J. H.; Chen, Y.-S.; Sengupta, D.; Thompson, R. R.; Powers, D. C. Oxygen-Atom Transfer Photochemistry of a Molecular Copper Bromate Complex. *Chem. Commun*. **2022**, *58*, 12608–12611.

(48) Betley, T. A.; Wu, Q.; Van Voorhis, T.; Nocera, D. G. Electronic Design Criteria for O–O Bond Formation via Metal–Oxo Complexes. *Inorg. Chem.* **2008**, *47*, 1849–1861.

(49) Gardner, J. G.; Schneider; J. E. Anderson, J. S. Two, Three, or Not to Be? Elucidating Multiple Bonding in $d^6$ Pseudotetrahedral Oxo and Imide Complexes. *Inorg. Chem.* **2021**, *18*, 13854–13860.

(50) Trofimenko, S. *Scorpionates: Polypyrazolylborate Ligands and Their Coordination Chemistry*, 1st ed.; Imperial College Press, 1999.

(51) Qiu, D.; Kilpatrick, L.; Kitajima, N.; Spiro, T. G. Modeling Blue Copper Protein Resonance Raman Spectra with Thiolate-$Cu^{II}$ Complexes of a Sterically Hindered Tris(pyrazolyl)borate. *J. Am. Chem. Soc.* **1994**, *116*, 2585–2590.

(52) Harding, D. J.; Phonsri, W.; Harding, P.; Sirirak, J.; Tangtirungrotechai, Y.; Webster, R. D.; Adams, H. Copper Hydrotris(3,5-diphenylpyrazolyl)borate Dithiocarbamates: Mimicking Green Copper Proteins. *New J. Chem.* **2015**, *39*, 1498–1505.

(53) Wurzenberger, M. H. H.; Szimhardt, N.; Stierstorfer, J. Copper(II) Chlorate Complexes: The Renaissance of a Forgotten and Misjudged Energetic Anion. *J. Am. Chem. Soc.* **2018**, *140*, 3206–3209.

(54) Garribba, E.; Micera, G. The Determination of the Geometry of Cu(II) Complexes: An EPR Spectroscopy Experiment. *J. Chem. Ed.* **2006,** *83*, 1229–1232.

(55) Katagiri, T.; Uneyama, K. Relative Gas Solubilities Correlate Linearly to the Refractive Indices of Aprotic Solvents. *Bull. Chem. Soc. Jpn.* **2010**, *83*, 788–789.

(56) Takaki, K.; Yamamoto, J.; Komeyama, K.; Kawabata, T.; Takehira, K. Photocatalytic Oxidation of Alkanes with Dioxygen by Visible Light and Copper(II) and Iron(III) Chlorides: Preference Oxidation of Alkanes over Alcohols and Ketones. *Bull. Chem. Soc. Jpn*. **2004**, *77*, 2251–2255.

(57) Ohkubo, K.; Hirose, K. Light-Driven C–H Oxygenation of Methane into Methanol and Formic Acid by Molecular Oxygen Using a Perfluorinated Solvent. *Angew. Chem. Int. Ed.* **2018,** *57*, 2126–2129.

(58) Zuo, Z.; Katsumura, Y.; Ueda, K.; Ishigure, K. Laser Photolysis Study on Reactions of Sulfate Radical and Nitrate Radical with Chlorate Ion in Aqueous Solutions Formation and Reduction Potential of $ClO_3$ Radical. *J. Chem. Soc., Faraday Trans.* **1997**, *93*, 533–536.

(59) Vilella, L.; Conde, A.; Balcells, D.; Díaz-Requejo, M. M.; Lledós, A.; Pérez, P. J. A Competing, Dual Mechanism for Catalytic Direct Benzene Hydroxylation from Combined Experimental-DFT Studies. *Chem. Sci.* **2017**, *8*, 8373–8383.

(60) Olivos-Suarez, A. I.; Szécsényi, À.; Hensen, E. J. M.; Ruiz-Martinez, J.; Pidko, E. A.; Gascon, J. Strategies for the Direct Catalytic Valorization of Methane Using Heterogeneous Catalysis: Challenges and Opportunities. *ACS Catal.* **2016**, *6*, 2965–2981.

*TOC*